Dimensional Crossover of Charge-Density Wave Correlations in the Cuprates

Yosef Caplan and Dror Orgad
Racah Institute of Physics, The Hebrew University, Jerusalem 91904, Israel
(Received 5 May 2017; published 8 September 2017)

Short-range charge-density wave correlations are ubiquitous in underdoped cuprates. They are largely confined to the copper-oxygen planes and typically oscillate out of phase from one unit cell to the next in the c direction. Recently, it was found that a considerably longer-range charge-density wave order develops in $YBa_2Cu_3O_{6+x}$ above a sharply defined crossover magnetic field. This order is more three-dimensional and is in-phase along the c axis. Here, we show that such behavior is a consequence of the conflicting ordering tendencies induced by the disorder potential and the Coulomb interaction, where the magnetic field acts to tip the scales from the former to the latter. We base our conclusion on analytic large-N analysis and Monte Carlo simulations of a nonlinear sigma model of competing superconducting and charge-density wave orders. Our results are in agreement with the observed phenomenology in the cuprates, and we discuss their implications to other members of this family, which have not been measured yet at high magnetic fields.

DOI: 10.1103/PhysRevLett.119.107002

The cuprate high-temperature superconductors are in a delicate state of balance between various electronic orders [1]. In particular, experiments have revealed a subtle interplay between the superconducting (SC) and charge-density wave (CDW) orders. Much of the evidence for the latter, coming from x-ray scattering [2–18] and nuclear magnetic resonance (NMR) measurements [19], points at short-range, in-plane, CDW order which is in competition with superconductivity. Concretely, the intensity of the CDW scattering peak grows as the system is cooled towards the SC transition temperature, T_c, and then decreases or saturates upon entering the SC phase. Furthermore, the CDW signal is enhanced when a magnetic field is used to partially quench superconductivity.

However, recent x-ray scattering measurements of $YBa_2Cu_3O_{6+x}$ (YBCO) [20–22] have detected additional Bragg peaks that are different in several respects from the signal described above. First, the new peaks are much sharper, thus corresponding to considerably longer-ranged CDW correlations. Second, whereas both the short-range and long-range CDW peaks share the same incommensurate in-plane wave vector, the latter appear only along the b direction and at integer c-axis wave vectors (measured in reciprocal lattice units), l. This stands in contrast to the bidirectional nature and the half-integer l of the former. Third, as also found by NMR [23,24] and ultrasound measurements [25], the longer-range CDW order sets in only above a magnetic field $H_{3D} \approx 15$ T, and at temperatures below $T_{3D} \approx 50$ K. The short-range correlations, however, appear already at zero field and survive up to about $T_{ch} = 150$ K.

Previously, aspects of competing SC and CDW orders were studied via Ginzburg-Landau and nonlinear sigma models (NLSMs) [26–33]. Those directly related to recent experiments include the CDW temperature dependence [29], the effects of disorder [30,31], and of a magnetic field [31–33]. However, a framework in which to understand the complete phenomenology, especially the relation between short- and long-range CDW order in YBCO, is lacking. Here, we offer such a scheme by including in our recent NLSM [31] the structure and couplings of YBCO, by elucidating the different effects of the disorder on the chain layers and on the CuO_2 planes, and by going beyond the interplane mean-field approximation. The gained insights are then applied to other cuprates.

We use analytical large-N and replica techniques alongside Monte Carlo (MC) simulations to show that the physics is driven by opposing forces. While the Coulomb interaction causes the CDW order to change sign from one plane to the next within a CuO_2 bilayer, its relative phase between consecutive unit cells in the c direction is frustrated. On the one hand, the disordered dopant potential on the chain layer tends to induce the same CDW configuration on the two adjacent CuO_2 bilayers. On the other hand, such an arrangement is costly from the point of view of their mutual capacitive energy, which is minimized by having them host out-of-phase CDWs.

At zero magnetic field the disorder prevails. CDW puddles that nucleate at locally favorable potential regions on the nearest CuO_2 planes to the chain layer tend to be in phase to each other and opposite to the CDW order that develops on the other CuO_2 plane within their bilayer. This leads to a CDW structure factor that is centered near half-integer l with a c-axis correlation length, ξ_c, of about one lattice constant. The in-plane correlation lengths, $\xi_{a,b}$, are longer but still extend over only few wave periods. For disorder fluctuations that are larger than the slight anisotropy induced by the chains, which benefits b-axis CDW, the nucleated CDW regions are distributed evenly between the a and b directions, thus leading to scattering peaks in both directions [34,35].

A magnetic field introduces vortices into the system at which superconductivity is suppressed and the CDW amplitude is significantly larger than its typical value without the field [36]. This in turn implies that the interlayer Coulomb interaction and the chain-induced anisotropy play a more important role in the energetic balance governing these regions. As an outcome, the CDW halos formed around a vortex line tend to order with integer l in the c direction and orient preferentially, although not exclusively, along the b axis. The disorder, on its part, interferes with the establishment of interhalo coherence, both along the vortex and, more importantly, between different vortices. However, as the field is made stronger, vortices move closer together until correlations between the b-oriented halos start rapidly increasing. Our calculations indicate that this growth would eventually turn into true long-range order at a critical field. Such a transition is possible since the chain disorder couples to the gradient of the integer-l CDW order, thereby reducing the lower critical dimension to $d_L = 2$. In contrast, any disorder on the CuO_2 layers, for which $d_L = 4$ [37], would smear the transition into a crossover. Nevertheless, as long as this disorder is not too strong the high-field state will still exhibit unidirectional integer-l CDW correlations persisting over long distances in all three dimensions.

The model.—Our NLSM of YBCO consists of N_c bilayers, see Fig. 1, hosting complex SC and CDW order parameters, $\psi_{\mu j}(\mathbf{r})$ and $\Phi^{a,b}_{\mu j}(\mathbf{r})$. The latter describe density variations $\delta\rho_{\mu j} = e^{i\mathbf{Q}_a\cdot\mathbf{r}}\Phi^a_{\mu j}(\mathbf{r}) + e^{i\mathbf{Q}_b\cdot\mathbf{r}}\Phi^b_{\mu j}(\mathbf{r}) + \text{c.c.}$, along the a and b directions with incommensurate wave vectors $\mathbf{Q}_{a,b}$. Here, j is the bilayer index and $\mu = 0, 1$ corresponds to the bottom (top) layer within a bilayer. Focusing on $T < T_{\text{ch}}$, we assume the existence of some type of local order and the competition between its components, as encapsulated by the constraints [29–31]

$$|\psi_{\mu j}|^2 + |\mathbf{\Phi}_{\mu j}|^2 = 1, \tag{1}$$

where $\mathbf{\Phi}_{\mu j} = (\Phi^a_{\mu j}, \Phi^b_{\mu j})^T$. The Hamiltonian reads

$$\begin{aligned} H = \sum_{\mu=0,1}\sum_{j=1}^{N_c} H_{\mu j} + \frac{\rho_s}{2}\sum_{j=1}^{N_c}\int d^2r[&\tilde{U}\mathbf{\Phi}^\dagger_{0j}\mathbf{\Phi}_{1j} \\ &+ U\mathbf{\Phi}^\dagger_{1j}\mathbf{\Phi}_{0j+1} - \tilde{J}\psi^*_{0j}\psi_{1j} - J\psi^*_{1j}\psi_{0j+1} \\ &+ \boldsymbol{V}^\dagger_j(\gamma\mathbf{\Phi}_{0j} + \mathbf{\Phi}_{1j} + \mathbf{\Phi}_{0j+1} + \gamma\mathbf{\Phi}_{1j+1}) + \text{H.c.}], \end{aligned} \tag{2}$$

with the SC stiffness, ρ_s, setting the overall energy scale. We model the Coulomb interaction between CDW fields within a bilayer by a local coupling $\tilde{U}$, and denote the intrabilayer Josephson tunneling amplitude by $\tilde{J}$. The (weaker) Coulomb interaction and Josephson coupling between nearest-neighbor CuO_2 layers belonging to adjacent unit cells are denoted by U and J, respectively. The disorder due to the doped oxygens on the chain layers

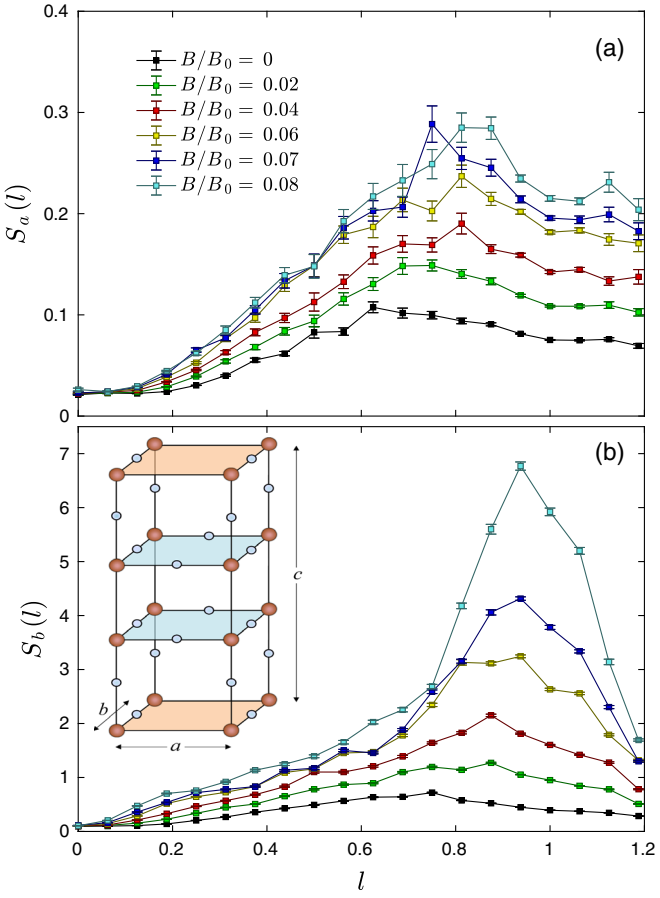

FIG. 1. The CDW structure factor at the a and b incommensurate peaks as function of c-axis wave vector, l, for $T = 0.2\rho_s$ and various magnetic fields. The inset depicts the YBCO unit cell. Only copper atoms (brown balls) and oxygen atoms (blue balls) are shown. The CuO_2 planes (light blue) host the SC and CDW orders. The doped oxygens go into the (orange) CuO_x chain layers and are the main source of disorder.

couples via Coulomb interaction to the CDW fields. We include its interaction with the neighboring bilayers, assuming that the coupling to the outer CuO_2 planes is reduced by a factor γ compared to the coupling to the inner CuO_2 planes. The disorder is described by independent random Gaussian fields $\boldsymbol{V}_j = (V^1_j + iV^2_j, V^3_j + iV^4_j)^T$, satisfying $\overline{V^\alpha_j(\mathbf{r})} = 0$ and $\overline{V^\alpha_j(\mathbf{r})V^\beta_{j'}(\mathbf{r}')} = V^2\delta_{\alpha\beta}\delta_{jj'}\delta(\mathbf{r}-\mathbf{r}')$, with the overline signifying disorder averaging. Within a layer the physics is governed by

$$\begin{aligned} H_{\mu j} = \frac{\rho_s}{2}\int d^2r[&|(\boldsymbol{\nabla} + 2ie\mathbf{A})\psi_{\mu j}|^2 + \lambda|\boldsymbol{\nabla}\mathbf{\Phi}_{\mu j}|^2 \\ &+ g|\mathbf{\Phi}_{\mu j}|^2 + \Delta g|\Phi^a_{\mu j}|^2 + (\tilde{\boldsymbol{V}}^\dagger_{\mu j}\mathbf{\Phi}_{\mu j} + \text{H.c.})], \end{aligned} \tag{3}$$

where $\lambda\rho_s$ is the CDW stiffness and $g\rho_s$ is the energy density penalty for CDW ordering. The Δg term reflects our assumption that the chain potential favors ordering along the b axis, either directly or via amplification by nematic

interactions between the CDW components [29,30,38]. We consider the extreme type-II limit where the magnetic field, B, is uniform and points in the c direction. Therefore, we include only its orbital coupling to the SC order. Finally, $\tilde{V}_{\mu j}$ is the disorder potential on the CuO_2 layers, which we model by Gaussian random fields with zero mean and $\overline{\tilde{V}^{\alpha}_{\mu j}(\mathbf{r})\tilde{V}^{\beta}_{\mu' j'}(\mathbf{r}')} = \tilde{V}^2\delta_{\alpha\beta}\delta_{\mu\mu'}\delta_{jj'}\delta(\mathbf{r}-\mathbf{r}')$.

Zero field.—Our main interest lies in k-space (measured from $\mathbf{Q}_{a,b}$) CDW correlations encapsulated by the matrix

$$G^{\alpha}_{\mu\mu'}(\mathbf{q},l) = \frac{1}{2N_c A}\int d^2r d^2r' \sum_{jj'} e^{-i[\mathbf{q}\cdot(\mathbf{r}-\mathbf{r}')+2\pi(j-j')l]} \times \overline{\langle \Phi^{\alpha}_{\mu j}(\mathbf{r})\Phi^{*\alpha}_{\mu' j'}(\mathbf{r}')\rangle}, \quad (4)$$

with A the layer area. To make analytical progress we increase the number of independent components of $\Phi^{a,b}$ from two to large $N/2$, assume $T \ll \rho_s$, and use a saddle-point approximation [39]. For $B=0$, and $\gamma = \tilde{V}^2 = 0$, $U \ll \tilde{U}$ we find (see Ref. [39] for the general result)

$$G^{\alpha}_{00}(0,l) = G^{\alpha}_{11}(0,l) = \frac{T}{\rho_s}\frac{\epsilon_\alpha}{\epsilon_\alpha^2 - \epsilon_\perp^2(l)} + \frac{V^2}{[\epsilon_\alpha + \epsilon_\perp(l)]^2} + \frac{4V^2\epsilon_\alpha\tilde{U}\sin^2\pi l}{[\epsilon_\alpha^2 - \epsilon_\perp^2(l)]^2}, \quad (5)$$

$$G^{\alpha}_{01}(0,l) = G^{*\alpha}_{10}(0,l) = -\frac{T}{\rho_s}\frac{\tilde{U}}{\epsilon_\alpha^2 - \epsilon_\perp^2(l)} + V^2\frac{[(\epsilon_\alpha - \tilde{U})\cos\pi l - i(\epsilon_\alpha + \tilde{U})\sin\pi l]^2}{[\epsilon_\alpha^2 - \epsilon_\perp^2(l)]^2}, \quad (6)$$

where $\epsilon_\alpha = g + \Delta g\delta_{\alpha a} + J + \tilde{J}$, and $\epsilon_\perp(l) = [U^2 + \tilde{U}^2 + 2U\tilde{U}\cos 2\pi l]^{1/2}$. Two ordering tendencies are apparent in Eqs. (5),(6). While the temperature terms reach a maximum at integer l, the disorder terms peak at half-integer l as long as $\epsilon_\alpha > 3U + \tilde{U}$, and dominate the correlation matrix if $V^2 > 2UT/\rho_s$, which is our case of interest. A small $\Delta g/g$ makes $\epsilon_a > \epsilon_b$ and introduces a slight tendency towards ordering along the b axis.

To go beyond the limitations of the saddle-point approximation we used MC simulations of the lattice version of Eqs. (1)–(3). The results are for a system of size $64\times64\times32$ (16 bilayers), which is open in the a direction, periodic in the b and c directions and whose parameters are $ga_0^2 = 1.1$, $\Delta g a_0^2 = 0.1$, $\tilde{J}a_0^2 = 0.15$, $Ja_0^2 = 0.015$, $\tilde{U}a_0^2 = 0.85$, $Ua_0^2 = 0.12$, $V^2a_0^2 = 0.1$, $\gamma = 0.15$, $\lambda = 1$. Here, a_0 is the in-plane lattice constant of the coarse grained model, which we assume is roughly the observed CDW wavelength, i.e., about 3 Cu-Cu spacings. Each data point was averaged over 50–70 disorder realizations [39].

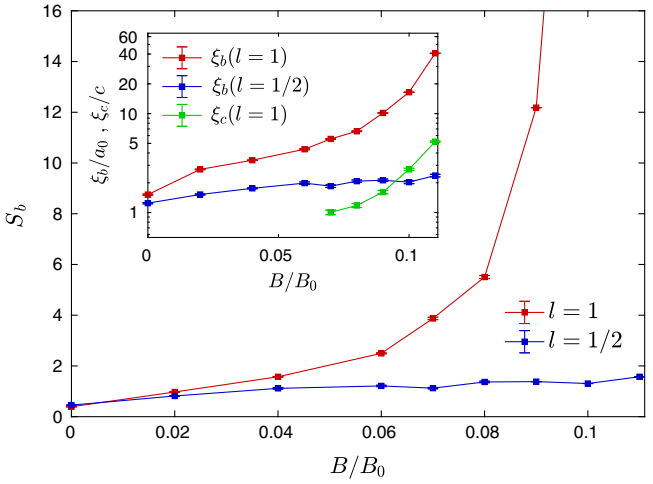

FIG. 2. A magnetic field strongly enhances the $l=1$ CDW structure factor peak in the b direction but only weakly affects the $l=1/2$ signal. Inset: in-plane, ξ_b, and out-of-plane, ξ_c, correlation lengths. Results are for $T = 0.2\rho_s$.

In order to establish contact with the x-ray scattering experiments we obtained the CDW structure factor $S_\alpha(\mathbf{q},l)$ by convolving G with the measured CDW form factors [17,39]. Figure 1 depicts the l dependence of the structure factor at the in-plane peaks $S_{a,b}(l) = S_{a,b}(0,l)$. We find that for $B=0$ both S_a and S_b exhibit a broad maximum centered around $l = 0.6$–0.7, whose asymmetry is largely due to the l dependence of the form factors. The correlation lengths $\xi_{b,c} = 1/\sigma_{b,c}$, extracted from fits to $e^{-q^2/2\sigma^2}$, are both of order one lattice constant, see Fig. 2, and the peak height reaches a maximum slightly above $T_c \simeq 0.42\rho_s$, see Fig. 3(a), all qualitatively consistent with experiments.

The effects of B.—The suppression of superconductivity inside magnetically induced vortices facilitates CDW nucleation there. At low B these localized modes form a narrow

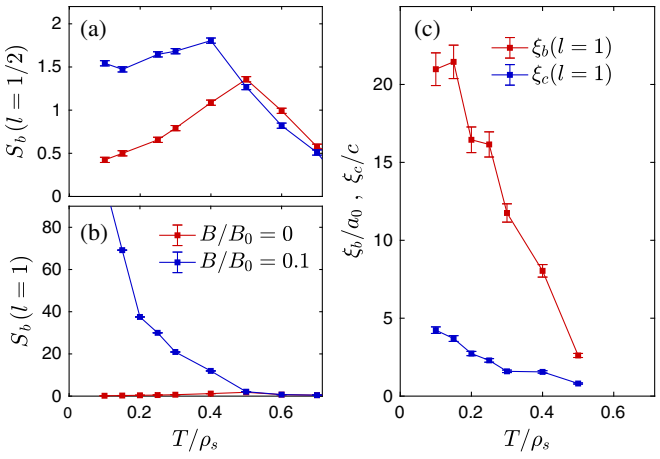

FIG. 3. (a) Low-temperature high-field saturation of the $l=1/2$ CDW b-peak vs (b) increase of the $l=1$ signal. (c) In-plane and out-of-plane $l=1$ correlation lengths at $B = 0.1B_0$.

band due to their small overlap and appear in tandem with the more extended CDW states, which are already present at $B = 0$ and produce the $l = 1/2$ correlations. Their contribution to G is similar to Eqs. (5),(6) apart of two modifications that determine its B dependence [39]. First is an overall B-linear factor reflecting the number of vortices. Second, ϵ_α is given by the bottom of the vortex band, which drifts down with B as CDW halos move closer together. Consequently, the maximum of the disorder terms shifts towards integer l and the entire G increases in magnitude. The effect, however, is very sensitive to the small anisotropy, Δg. Our MC results, shown in Figs. 1 and 2, demonstrate that the CDW core regions orient predominantly along the b axis, causing S_b to form a rapidly growing peak near $l = 1$ for fields beyond $B_{3D} = 0.06$–$0.07B_0$. Since $B_0 = \phi_0/2\pi a_0^2 \simeq 250$ T, where $\phi_0 = \pi/e$ is the flux quantum, this crossover scale corresponds to 15–18 T for the set of parameters used by us. At the same time Fig. 1 shows that S_a is only weakly modified by the presence of the field.

The agreement of the calculated high-field signal with the observed x-ray phenomenology [20–22] extends beyond its unidirectionality and sharp B dependence. Figure 2 shows that the increase of $S_b(l = 1)$ is accompanied by a substantial growth of the $l = 1$ correlation lengths. At $B = 0.11B_0$, the highest field we could handle without significant finite-size effects, ξ_c extends over five c-axis lattice constants and $\xi_b = 40a_0$ is found within the planes. In contrast, the $l = 1/2$ correlation lengths change very little with B and remain short. The dichotomy between the two types of correlations is also reflected by their T dependence, depicted in Fig. 3. While the $T = 0.5\rho_s$ peak of the $l = 1/2$ signal turns into a low-temperature saturation in the presence of high magnetic fields [3], $S_b(l = 1)$ and its associated correlation lengths exhibit a rapid upturn below $T_{3D} = 0.5\rho_s$ at large B.

Transition to long-range order.—The following Imry-Ma argument [37] shows that in the absence of in-plane disorder the integer-l CDW can become long-ranged. Consider a domain of linear size L of such a CDW. If the order is constant, the interaction of the chain disorder with its neighboring CuO_2 planes cancels out. However, if the order varies as $1/L$ along the c axis, the averaged squared interaction scales, in d dimensions, as L^{d-2} and can lead to a typical energy gain of $L^{d/2-1}$. Since the elastic energy to create the domains scales as L^{d-2} their proliferation become favorable only in $d \leq 2$. Our large-N analysis reflects this physics [39]. For $\tilde{V}^2 = 0$ and $V^2 \ll (r_0 U)^2 < U \ll \tilde{U}$ we find that ξ_c diverges at

$$\frac{T_{\mathrm{CDW}}}{\rho_s} = \kappa r_0^2 \sqrt{tU} - \frac{V^2}{2U}, \tag{7}$$

where r_0 is the vortex core radius, $t \sim r_0^{-2} e^{-b\sqrt{\phi_0/Br_0^2}}$ and κ, b are constants. Hence, the clean system orders for any small magnetic field at low-enough temperatures. In the presence of chain disorder a transition occurs only above a critical field, which for $T = 0$ is approximately

$$\frac{B_{\mathrm{CDW}} r_0^2}{\phi_0} \approx \ln^{-2}\left[\kappa^2 r_0^2 U \left(\frac{2U}{V^2}\right)^2\right]. \tag{8}$$

Similar expressions for the case of stronger disorder can be found in Ref. [39].

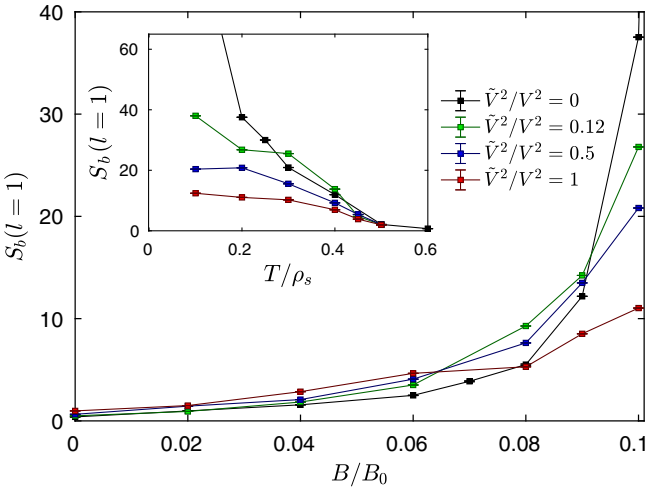

FIG. 4. Suppression of the $l = 1$ CDW b peak by in-plane disorder, $\tilde{V}$, as revealed by its dependence on magnetic field (at $T = 0.2\rho_s$) and on temperature (at $B = 0.1B_0$).

The effects of in-plane disorder.—Contrary to the chain disorder, the in-plane disorder couples to each layer separately, leads to a typical energy gain which scales as $L^{d/2}$, and thus prevents long-range order at $d \leq 4$ [37]. Indeed, our saddle-point equations [39] do not admit a diverging ξ_c when $\tilde{V}^2 > 0$. Figure 4 shows that as $\tilde{V}^2/V^2$ approaches 1 the rapid increase of the $l = 1$ correlations is averted. We therefore infer that in the physical systems $\tilde{V}^2 \ll V^2$.

The sensitivity to Δg.—It is difficult to ascertain the magnitude of the anisotropy in g. A proxy might be the resistivity anisotropy, which is roughly $\rho_a/\rho_b \approx 1.5$ in the relevant YBCO samples [40]. Much larger values have been measured for the ratio of the Nernst coefficients [41]. The presented MC results are for $\Delta g/g = 9\%$ and we have checked that deviations from a unidirectional $l = 1$ signal commence only around $\Delta g/g = 3\%$.

Discussion.—Let us conclude by pointing out few consequences of our model. First, since the enhancement of CDW by a magnetic field is driven by the suppression of superconductivity, one is led to infer the existence of local SC order as long as CDW correlations continue to increase with B. Surprisingly, in ortho-VIII YBCO [22] the $l = 1$ scattering intensity and correlation volume grow up to $H = 32$ T, well in excess of the resistive critical field $H_{c2} = 24$ T [42]. Hence, an interesting possibility arises

that in this system local SC order continues to exist long after global superconductivity is lost.

Secondly, like in YBCO the disorder due to doped oxygens in $HgBa_2CuO_{4+\delta}$ resides on planes (HgO) [13] shared by consecutive unit cells along the c axis. The arguments presented above would then imply that in this single-layer compound low-field CDW correlations should broadly peak near integer l. Zero-field measurements [12] found CDW peaks at $l = 1.12$ and $l = 1.25$, but experimental constraints make it currently impossible to determine whether these are the true maxima. In a magnetic field the interaction between CDW halos on neighboring planes is expected to move the scattering peaks towards half-integer l. Since $HgBa_2CuO_{4+\delta}$ is tetragonal, with no dopant order or signs of nematicity, the signal would likely remain bidirectional. On the other hand, in the $La_{2-x}Sr_xCuO_4$ unit cell, each of the two CuO_2 planes is separately affected, at least to first approximation, by the Sr disorder on its adjacent LaO layers. Furthermore, consecutive CuO_2 planes are offset by half a lattice constant and Coulomb interactions between next-nearest-neighbor planes dominate and lead to half-integer-l peaks at low fields [10,11]. We then expect a high field to strengthen and sharpen the peaks without shifting their l.

This research was supported by the Israel Science Foundation (Grant No. 701/17) and by the United States-Israel Binational Science Foundation (Grant No. 2014265).

[1] E. Fradkin, S. A. Kivelson, and J. M. Tranquada, Colloquium: Theory of intertwined orders in high temperature superconductors, Rev. Mod. Phys. **87**, 457 (2015).

[2] G. Ghiringhelli *et al.*, Long-range incommensurate charge fluctuations in $(Y,Nd)Ba_2Cu_3O_{6+x}$, Science **337**, 821 (2012).

[3] J. Chang, E. Blackburn, A. T. Holmes, N. B. Christensen, J. Larsen, J. Mesot, R. Liang, D. A. Bonn, W. N. Hardy, A. Watenphul, M. v. Zimmermann, E. M. Forgan, and S. M. Hayden, Direct observation of competition between superconductivity and charge density wave order in $YBa_2Cu_3O_{6.67}$, Nat. Phys. **8**, 871 (2012).

[4] A. J. Achkar, R. Sutarto, X. Mao, F. He, A. Frano, S. Blanco-Canosa, M. Le Tacon, G. Ghiringhelli, L. Braicovich, M. Minola, M. Moretti Sala, C. Mazzoli, R. Liang, D. A. Bonn, W. N. Hardy, B. Keimer, G. A. Sawatzky, and D. G. Hawthorn, Distinct Charge Orders in the Planes and Chains of Ortho-III-Ordered $YBa_2Cu_3O_{6+\delta}$ Superconductors Identified by Resonant Elastic X-Ray Scattering, Phys. Rev. Lett. **109**, 167001 (2012).

[5] E. Blackburn, J. Chang, and M. Hücker, A. T. Holmes, N. B. Christensen, R. Liang, D. A. Bonn, W. N. Hardy, U. Rütt, O. Gutowski, M. v. Zimmermann, E. M. Forgan, and S. M. Hayden, X-Ray Diffraction Observations of a Charge-Density-Wave Order in Superconducting Ortho-II $YBa_2Cu_3O_{6.54}$ Single Crystals in Zero Magnetic Field, Phys. Rev. Lett. **110**, 137004 (2013).

[6] A. J. Achkar, X. Mao, C. McMahon, R. Sutarto, F. He, R. Liang, D. A. Bonn, W. N. Hardy, and D. G. Hawthorn, Impact of Quenched Oxygen Disorder on Charge Density Wave Order in $YBa_2Cu_3O_{6+x}$, Phys. Rev. Lett. **113**, 107002 (2014).

[7] R. Comin, A. Frano, M. M. Yee, Y. Yoshida, H. Eisaki, E. Schierle, E. Weschke, R. Sutarto, F. He, A. Soumyanarayanan, Yang He, M. Le Tacon, I. S. Elfimov, J. E. Hoffman, G. A. Sawatzky, B. Keimer, and A. Damascelli, Charge order driven by Fermi-arc instability in $Bi_2Sr_{2-x}La_xCuO_{6+\delta}$, Science **343**, 390 (2014).

[8] E. H. da Silva Neto, P. Aynajian, A. Frano, R.Comin, E. Schierle, E. Weschke, A. Gyenis, J. Wen, J. Schneeloch, Z.Xu, S. Ono, G. Gu, M. Le Tacon, and A. Yazdani, Ubiquitous interplay between charge ordering and high-temperature superconductivity in cuprates, Science **343**, 393 (2014).

[9] M. Le Tacon, A. Bosak, S. M. Souliou, G. Dellea, T. Loew, R. Heid, K.-P. Bohnen, G. Ghiringhelli, M. Krisch, and B. Keimer, Inelastic x-ray scattering in $YBa_2Cu_3O_{6.6}$ reveals giant phonon anomalies and elastic central peak due to charge-density-wave formation, Nat. Phys. **10**, 52 (2014).

[10] T. P. Croft, C. Lester, M. S. Senn, A. Bombardi, and S. M. Hayden, Charge density wave fluctuations in $La_{2-x}Sr_xCuO_4$ and their competition with superconductivity, Phys. Rev. B **89**, 224513 (2014).

[11] N. B. Christensen, J. Chang, J. Larsen, M. Fujita, M. Oda, M. Ido, N. Momono, E. M. Forgan, A. T. Holmes, J. Mesot, M. Huecker, and M. v. Zimmermann, Bulk charge stripe order competing with superconductivity in $La_{2-x}Sr_xCuO_4$ ($x = 0.12$), arXiv:1404.3192.

[12] W. Tabis *et al.*, Charge order and its connection with Fermi-liquid charge transport in a pristine high-T_c cuprate, Nat. Commun. **5**, 5875 (2014).

[13] G. Campi, A. Bianconi, N. Poccia, G. Bianconi, L. Barba, G. Arrighetti, D. Innocenti, J. Karpinski, N. D. Zhigadlo, S. M. Kazakov, M. Burghammer, M. v. Zimmermann, M. Sprung, and A. Ricci, Inhomogeneity of charge-density-wave order and quenched disorder in a high-T_c superconductor, Nature (London) **525**, 359 (2015).

[14] E. H. da Silva Neto, R. Comin, F. He, R. Sutarto, Y. Jiang, R. L. Greene, G. A. Sawatzky, and A. Damascelli, Charge ordering in the electron-doped superconductor $Nd_{2-x}Ce_xCuO_4$, Science **347**, 282 (2015).

[15] R. Comin, R. Sutarto, E. H. da Silva Neto, L. Chauviere, R. Liang,, W. N. Hardy, D. A. Bonn, F. He, G. A. Sawatzky, and A. Damascelli, Broken translational and rotational symmetry via charge stripe order in underdoped $YBa_2Cu_3O_{6+y}$, Science **347**, 1335 (2015).

[16] R. Comin, R. Sutarto, F. He, E. H. da Silva Neto, L. Chauviere, and A. Fraño, R. Liang, W. N. Hardy, D. A. Bonn, Y. Yoshida, H. Eisaki, A. J. Achkar, D. G. Hawthorn, B. Keimer, G. A. Sawatzky, and A. Damascelli, Symmetry of charge order in cuprates, Nat. Mater. **14**, 796 (2015).

[17] E. M. Forgan, E. Blackburn, A. T. Holmes, A. K. R. Briffa, J. Chang, L. Bouchenoire, S. D. Brown, R. Liang, D. Bonn, W. N. Hardy, N. B. Christensen, M. v. Zimmermann, and M. Hücker, and S. M. Hayden, The microscopic structure of charge density waves in underdoped $YBa_2Cu_3O_{6.54}$ revealed by x-ray diffraction, Nat. Commun. **6**, 10064 (2015).

[18] Y. Y. Peng, M. Salluzzo, X. Sun, A. Ponti, D. Betto, A. M. Ferretti, F. Fumagalli, K. Kummer, M. Le Tacon, X. J. Zhou, N. B. Brookes, L. Braicovich, and G. Ghiringhelli, Direct observation of charge order in underdoped and optimally doped $Bi_2(Sr, La)_2CuO_{6+\delta}$ by resonant inelastic x-ray scattering, Phys. Rev. B **94**, 184511 (2016).

[19] T. Wu, H. Mayaffre, S. Krämer, M. Horvatić, C. Berthier, W. N. Hardy, R. Liang, D. A. Bonn, and M.-H Julien, Incipient charge order observed by NMR in the normal state of $YBa_2Cu_3O_y$, Nat. Commun. **6**, 6438 (2015).

[20] S. Gerber *et al.*, Three-dimensional charge density wave order in $YBa_2Cu_3O_{6.67}$ at high magnetic fields, Science **350**, 949 (2015).

[21] J. Chang, E. Blackburn, O. Ivashko, A. T. Holmes, N. B. Christensen, and M. Hücker, R. Liang, D. A. Bonn, W .N. Hardy, U. Rütt, M. v. Zimmermann, E. M. Forgan, and S. M. Hayden, Magnetic field controlled charge density wave coupling in underdoped $YBa_2Cu_3O_{6+x}$, Nat. Commun. **7**, 11494 (2016).

[22] H. Jang *et al.*, Ideal charge density wave order in the high-field state of superconducting YBCO, Proc. Natl. Acad. Sci. U.S.A. **113**, 14645 (2016).

[23] T. Wu, H. Mayaffre, S. Krämer, M. Horvatć, C. Berthier, W. N. Hardy, R. Liang, D. A. Bonn, and M.-H. Julien, Magnetic-field-induced charge-stripe order in the high-temperature superconductor $YBa_2Cu_3O_y$, Nature (London) **477**, 191 (2011).

[24] T. Wu, H. Mayaffre, S. Krämer, M. Horvatić, C. Berthier, P. L. Kuhns, A. P. Reyes, R. Liang, W. N. Hardy, D. A. Bonn, and M.-H. Julien, Emergence of charge order from the vortex state of a high-temperature superconductor, Nat. Commun. **4**, 2113 (2013).

[25] D. LeBoeuf and S. Krämer, W. N. Hardy, R. Liang, D. A. Bonn, and C. Proust, Thermodynamic phase diagram of static charge order in underdoped $YBa_2Cu_3O_y$, Nat. Phys. **9**, 79 (2013).

[26] O. Zachar, S. A. Kivelson, and V. J. Emery, Landau theory of stripe phases in cuprates and nickelates, Phys. Rev. B **57**, 1422 (1998).

[27] E. Demler and S. Sachdev, Competing orders in thermally fluctuating superconductors in two dimension, Phys. Rev. B **69**, 144504 (2004).

[28] K. B. Efetov, H. Meier, and C. Pépin, Pseudogap state near a quantum critical point, Nat. Phys. **9**, 442 (2013).

[29] L. E. Hayward, D. G. Hawthorn, R. G. Melko, and S. Sachdev, Angular fluctuations of a multicomponent order describe the pseudogap of $YBa_2Cu_3O_{6+x}$, Science **343**, 1336 (2014).

[30] L. Nie, L. E. Hayward Sierens, R. G. Melko, S. Sachdev, and S. A. Kivelson, Fluctuating orders and quenched randomness in the cuprates, Phys. Rev. B **92**, 174505 (2015).

[31] Y. Caplan, G. Wachtel, and D. Orgad, Long-range order and pinning of charge-density waves in competition with superconductivity, Phys. Rev. B **92**, 224504 (2015).

[32] H. Meier, M. Einenkel, C. Pépin, and K. B. Efetov, Effect of magnetic field on the competition between superconductivity and charge order below the pseudogap state, Phys. Rev. B **88**, 020506(R) (2013).

[33] M. Einenkel, H. Meier, C. Pépin, and K. B. Efetov, Vortices and charge order in high-T_c superconductors, Phys. Rev. B **90**, 054511 (2014).

[34] A. Del Maestro, B. Rosenow, and S. Sachdev, From stripe to checkerboard ordering of charge-density waves on the square lattice in the presence of quenched disorder, Phys. Rev. B **74**, 024520 (2006).

[35] J. A. Robertson, S. A. Kivelson, E. Fradkin, A. C. Fang, and A. Kapitulnik, Distinguishing patterns of charge order: Stripes or checkerboards, Phys. Rev. B **74**, 134507 (2006).

[36] Indirect supporting evidence for this assertion comes from scanning tunneling microscopy of $Bi_2Sr_2CaCu_2O_{8+x}$, M. H. Hamidian, S. D. Edkins, K. Fujita, A. Kostin, A. P. Mackenzie, H. Eisaki, S. Uchida, M. J. Lawler, E.-A. Kim, S. Sachdev, and J. C. S. Davis, Magnetic-field induced interconversion of Cooper pairs and density wave states within cuprate composite order, arXiv:1508.00620.

[37] Y. Imry and S.-K. Ma, Random-Field Instability of the Ordered State of Continuous Symmetry, Phys. Rev. Lett. **35**, 1399 (1975).

[38] L. Nie, G. Tarjus, and S. A. Kivelson, Quenched disorder and vestigial nematicity in the pseudogap regime of the cuprates, Proc. Natl. Acad. Sci. U.S.A. **111**, 7980 (2014).

[39] See Supplemental Material at http://link.aps.org/supplemental/10.1103/PhysRevLett.119.107002 for details on the large-N analysis of the model, the relation of its correlation functions to the x-ray scattering experiments, and for an example of disorder averaging of the Monte Carlo data.

[40] Y. Ando, K. Segawa, S. Komiya, and A. N. Lavrov, Electrical Resistivity Anisotropy from Self-Organized One Dimensionality in High-Temperature Superconductors, Phys. Rev. Lett. **88**, 137005 (2002).

[41] R. Daou, J. Chang, D. LeBoeuf, and O. Cyr-Choinière, F. Laliberté, N. Doiron-Leyraud, B. J. Ramshaw, R. Liang, D. A. Bonn, W. N. Hardy, and L. Taillefer, Broken rotational symmetry in the pseudogap phase of a high-T_c superconductor, Nature (London) **463**, 519 (2010).

[42] G. Grissonnanche *et al.*, Direct measurement of the upper critical field in cuprate superconductors, Nat. Commun. **5**, 3280 (2014).